



ELSEVIER

Journal of Electron Spectroscopy and Related Phenomena 114–116 (2001) 93–97

---

---

**JOURNAL OF  
ELECTRON SPECTROSCOPY**  
and Related Phenomena

---

---

www.elsevier.nl/locate/elspec

# Generalized oscillator strength profiles for inner shell excitation of CO<sub>2</sub> derived from variable angle electron energy loss spectroscopy

T. Tyliczszak<sup>a</sup>, I.G. Eustatiu<sup>a</sup>, A.P. Hitchcock<sup>a,\*</sup>, C.C. Turci<sup>b</sup>, A.B. Rocha<sup>b</sup>,  
C.E. Bielschowsky<sup>b</sup>

<sup>a</sup>Department of Chemistry, McMaster University, Hamilton, ON, L8S 4M1, Canada

<sup>b</sup>Instituto de Química, Universidade Federal do Rio de Janeiro, Rio de Janeiro, RJ 21910, Brazil

Received 8 August 2000; received in revised form 2 October 2000; accepted 2 October 2000

---

## Abstract

GOS profiles for C 1s and O 1s excitation of CO<sub>2</sub> have been derived from inner shell electron energy loss spectra of CO<sub>2</sub> measured over a wide range of scattering angles (4–62°). The experimental profiles are compared to computed GOS profiles calculated within the first Born approximation, using ab-initio configuration interaction wave functions for the C 1s transitions and ab-initio generalized multi structural wave functions for the O 1s transitions. The theoretical and experimental results are in generally good agreement indicating that the first Born approximation holds to a surprisingly large momentum transfer for the core excitations studied. The computations predict there should be oscillations in the GOS for O 1s→nsσ<sub>g</sub> (536.5, 539 eV) and npσ<sub>u</sub> Rydberg states (~539 eV) but not for π symmetry states. Measurements with a newly installed parallel detector provide experimental support for the existence of oscillations in the GOS profile for the O 1s excitation of CO<sub>2</sub> at 539 eV. These oscillations may arise from interference between core excitations localized on the left or right oxygen atom of CO<sub>2</sub>. © 2001 Elsevier Science B.V. All rights reserved.

**Keywords:** CO<sub>2</sub>; Inner shell excitation; Generalized oscillator strength; Core hole localization

---

## 1. Introduction

In the regime of weak to moderate interaction, inelastic electron scattering can be treated in the Bethe–Born model, which describes the scattering intensities at a given momentum transfer in terms of a generalized oscillator strength (GOS). The generalized oscillator strength is a convenient way to

summarize the systematics of dipole and non-dipole electron impact electronic excitation. While the GOS profiles for valence electron excitation have been extensively explored, very few systematic studies of the GOS profiles of inner shell excitations have been reported. As part of such a systematic program we have measured the inner shell electron energy loss spectra of CO<sub>2</sub> in the region of C 1s and O 1s excitation over a wide range of scattering angles (out to 62°), corresponding to momentum transfers (*K*) as high as 8.4 a.u. [1]. This paper summarizes some of the highlights of that work, and extends it through a

---

\*Corresponding author. Tel.: +1-905-525-91450; fax: +1-905-521-2773.

E-mail address: aph@mcmaster.ca (A.P. Hitchcock).

higher statistical precision, parallel detection study of a weak oscillatory structure in one of the O 1s signals.

## 2. Experimental

Measurements were made with a variable impact energy, variable angle electron energy-loss spectrometer [2] operated with an unmonochromated beam, which provides 0.8 eV fwhm resolution. A collision cell was used to achieve higher target gas pressures and thus to enable detection of the weak signals at large momentum transfer. The pass energy for the analyzer was 50 eV and the final electron energy was 1300 eV. The spectrometer has been described in detail elsewhere [2]. A resistive anode parallel detector (Quantar 2502 position analyzer) has been installed recently and the high statistical precision O 1s measurement was used in part as a test of its capabilities.

The measured scattering intensities were normalized to incident current, gas pressure and time; corrected for variation of scattering geometry with scattering angle; and then converted to absolute GOS values by normalization of the  $\pi^*$  optical oscillator strength (GOS extrapolated to  $K=0$ ) to literature values [3]. Full details of the data acquisition, analysis procedures and systematic checks are provided elsewhere [1,2].

## 3. Theory

The generalized oscillator strength was calculated within the first Born approximation (FBA). The target electronic wave functions were determined independently for the ground and each excited state, using the configuration-interaction method (CI) for the C 1s transitions and generalized multi structural method (GMS) for the O 1s transitions. The molecular basis functions used in the CI and GMS calculations were Hartree–Fock molecular orbitals for the occupied states, and improved virtual orbitals for the virtual space, optimized independently for the ground and each excited state. In this way, relaxation, correlation and localization effects were explicitly taken into account.

## 4. Results

Fig. 1 compares a small angle, dipole regime C 1s spectrum of CO<sub>2</sub> to a large angle spectrum. The normalized signals were background subtracted and converted to a generalized oscillator strength scale. An additional weak, broad signal is detected around 298 eV at larger scattering angles, as is indicated by the broad maximum in the normalized ratio of the 28° and 4° spectra. This is assigned to the dipole forbidden C 1s $\sigma_g \rightarrow 5\sigma_g^*$  transition which had been predicted [4] but not observed prior to these measurements.

Fig. 2 presents the GOS profiles for the C 1s $\rightarrow\pi^*$  and 3p transitions in comparison to the theoretical GOS computed within the first Born approximation, using ab-initio configuration interaction wave functions. The GOS profile for the 5 $\sigma_g^*$  transition is also plotted. It is consistent with a dipole forbidden, quadrupole allowed transition. For most of the C 1s states the theoretical and experimental results are in

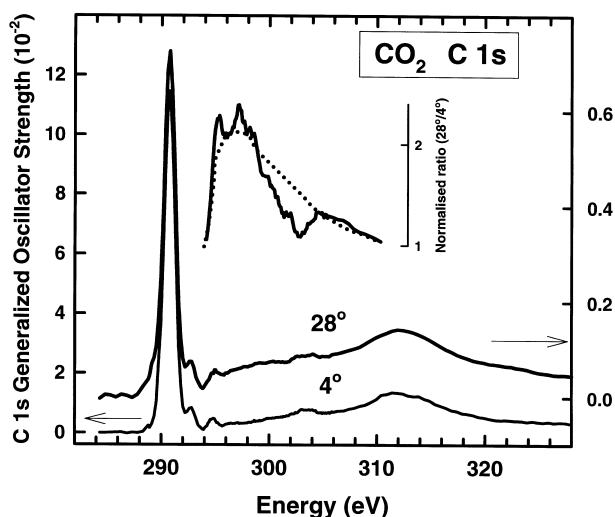


Fig. 1. Comparison of the C 1s spectrum of CO<sub>2</sub> at small and large momentum transfer. The measured inner shell energy loss (ISEELS) spectrum has been converted to an absolute GOS scale and the underlying valence contribution subtracted. The inset plots the ratio of the 28° to the 4° spectra (normalized to unit area of the  $\pi^*$  peak), in order to show more clearly the additional intensity around 298 eV which arises from the quadrupole allowed, dipole-forbidden, C 1s $\sigma_g \rightarrow 5\sigma_g^*$  transition. The dotted line sketches a possible line shape for the 5 $\sigma_g^*$  transition. The superimposed sharp structures arise from the  $K$ -dependence of 2-electron dipole transitions.

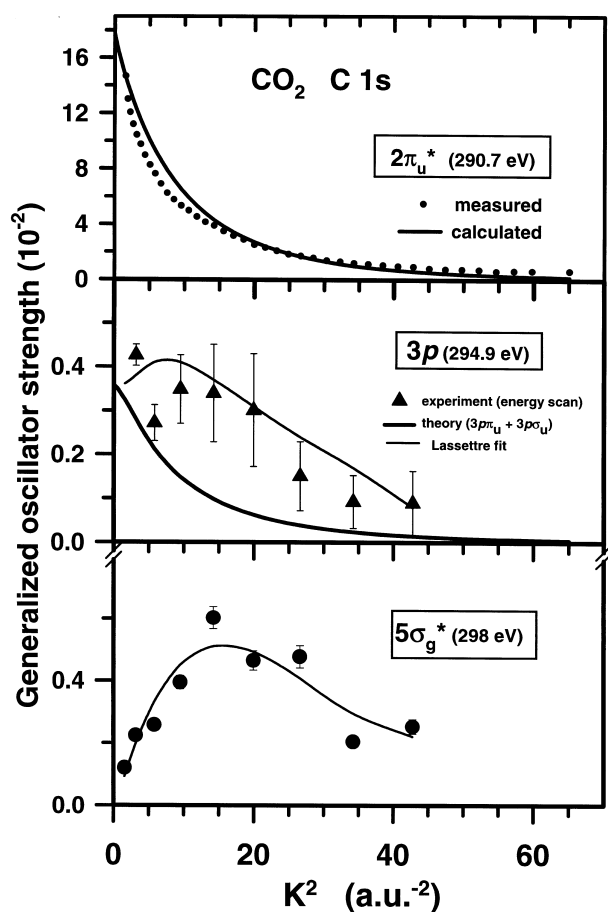


Fig. 2. GOS profiles for excitations to the  $2\sigma^*$ ,  $3p$  and  $5\sigma_g^*$  C  $1s$  excited states. The first two plots include a comparison to computed GOS, while the latter two plots also include Lassetre fits.

good agreement. In the valence excitation regime deviations from the first Born approximation are often apparent by  $K \sim 3$  a.u. [5,6]. The good agreement found in this work suggests that the first Born approximation holds to a rather large momentum transfer for core excitation. While at first surprising, this may be related simply to the fact that core orbitals are much smaller than valence orbitals. The more compact size means that a significantly smaller impact parameter, and thus higher momentum transfer must be reached before the strength of the electron-molecule interaction reaches the point where second Born terms become significant.

Fig. 3 compares the O  $1s$  spectra of  $\text{CO}_2$  recorded at  $4^\circ$  and  $28^\circ$ . Since all transitions are dipole allowed due to the existence of O  $1s$  levels of each parity, it

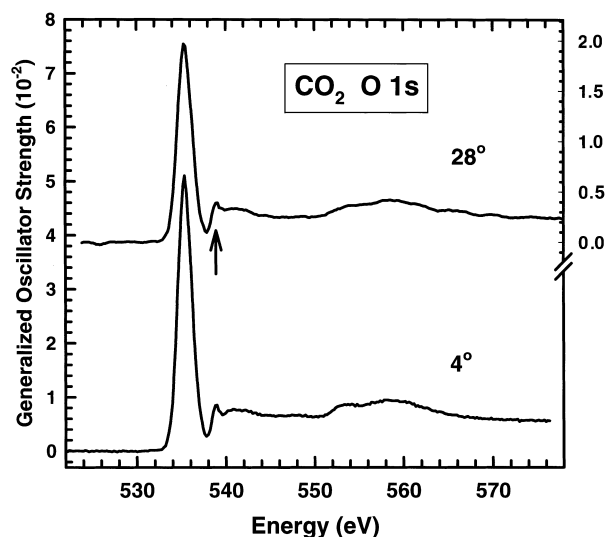


Fig. 3. Comparison of the O  $1s$  spectrum of  $\text{CO}_2$  at small and large momentum transfer. The underlying valence and C  $1s$  contributions have been subtracted from the measured inner shell energy loss (ISEELS) spectrum which has then been converted to an absolute GOS scale.

is perhaps not surprising that there is little *apparent* change in the shape of the O  $1s$  spectrum with momentum transfer. Fig. 4 compares the measured and computed GOS profiles for the O  $1s \rightarrow 2\pi^*$  state of  $\text{CO}_2$ . In this case the computed O  $1s$  GOS is based on ab initio generalized multi structural wave functions to properly account for the presence of two symmetry equivalent O atoms and the partial delocalization of the O  $1s$  core hole [7]. Theory predicts large quadrupole contributions to the GOS for almost all O  $1s$  excitations in  $\text{CO}_2$ . The level of agreement of theory and experiment indicated in Fig. 4 was only obtained after the experimental curve was normalized to theory in the low- $k$  region. There is a  $\sim 20\%$  deviation from theory when the experimental data extrapolated to  $K=0$  is normalized to optical values. We interpret this as evidence for a significant quadrupole contribution for O  $1s \rightarrow 2\pi^*$  excitation which turns on at low momentum transfer, as theory predicts [1]. It will be important in the future to make careful measurements of the GOS profile in the very low- $K$  region ( $K^2 < 4$  a.u. $^{-2}$ ) to see if the turn-over predicted by the computation is real (see insert to Fig. 4). The maximum in the computed total GOS occurs below the minimum  $K$  which we can access at the present time.

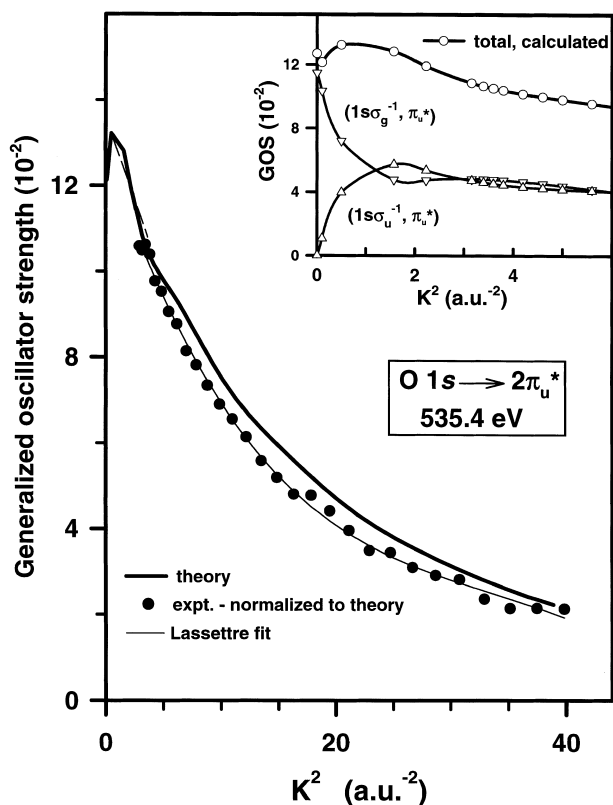


Fig. 4. GOS profiles for excitations to the  $2\sigma^*$  O  $1s$  excited state compared to the GOS profile computed using ab-initio generalized multi structural wave functions to represent the partial delocalization of the O  $1s$  core hole. The inset plots an expansion of the computed signals in the low- $K$  region to show the expected decrease of the computed quadrupole contribution as  $K \rightarrow 0$ .

The computed GOS profiles for the O  $1s \rightarrow ns\sigma$ ,  $np\sigma$  and  $np\pi$  Rydberg states (corresponding to experimental signals at 536 and 539 eV) are presented in Fig. 5a. The computed  $3s\sigma_g$  and  $4s\sigma_g$  GOS profiles exhibit oscillations with the same period and phase while the  $3p\sigma_u$  GOS profile exhibits oscillations of the same frequency, but of opposite phase. In contrast, the  $2\pi^*$  and  $3p\pi_u$  GOS profiles do not oscillate. The oscillations in the  $\sigma$ -channel excitations may arise from interference between core excitations localized on the left or right oxygen atom of  $\text{CO}_2$  [1]. If so, it would be a direct manifestation of coherency in electron scattering involving symmetry equivalent excitations such as the O  $1s$  core states. Such an effect was predicted by Karle and Swick more than 40 years ago in respect to valence excitations of  $\text{CCl}_4$  [8,9] and  $\text{Br}_2$  [10]. Later on, Lee

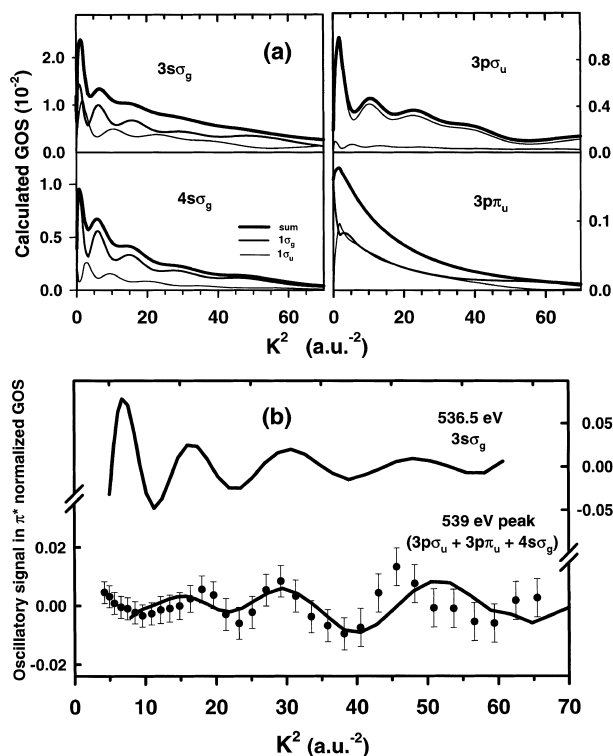


Fig. 5. (a) Computed GOS profiles for the  $3s\sigma_g$ ,  $4s\sigma_g$ ,  $3p\sigma_u$  and  $3p\pi_u$  O  $1s$  excited states. The dipole and quadrupole contributions are shown along with their sum. The sum is expected to be observed experimentally since the  $\sigma_g - \sigma_u$  separation is smaller than the O  $1s$  core state line width. (b) Comparison of computed and measured oscillatory components of the GOS for 539 eV (sum of  $4s\sigma_g$ ,  $3p\sigma_u$  and  $3p\pi_u$ ) state and the oscillatory component for the computed  $3s\sigma_g$  state (536.5 eV). Both computed and experimental oscillatory components were isolated by a 2-section cubic spline fit applied to the ratio of the indicated signals to the  $2\pi^*$  GOS profile, which does not oscillate, according to both theory and experiment. The oscillations isolated from the experimental signal was inverted and 3-point Savitsky-Golay smoothed.

et al. [11] presented new experimental results for valence-excited  $\text{CCl}_4$  and discussed the early results of Karle and Swick [8–10]. They concluded that the effects seen in  $\text{CCl}_4$  most probably were related to multiple scattering. However they also concluded that a correlation observed between elastic/inelastic features in  $\text{Br}_2$  could be related to coherent scattering, although it could also be a manifestation of the nodal structure of atomic-like Rydberg orbitals. Generalized oscillator strength oscillations related to the nodal structure of orbitals is clearly seen in electron impact excitation of atoms [7], where no

coherent scattering can take place. At present we are carrying out systematic computational studies to determine whether or not the computed oscillations are related to the use of GMS wave-functions for the O 1s calculations. By computing the GOS for the  $3s\sigma_g$  state with a non-GMS, core-hole localized CI wave-function it should be possible to gain insight into the origin of these oscillations.

Fig. 5b presents O 1s GOS measurements using the new parallel detector. In order to reduce the possibility of systematic error, the oscillations extracted from a 2-section cubic spline fit to the ratio of the experimental GOS for the 539 eV signal to that for the  $\pi^*$  peak, are plotted in comparison to the corresponding computational quantity, namely the oscillations extracted by the same spline procedure applied to the sum of the  $4s\sigma_g$ ,  $3p\sigma_u$ , and  $3p\pi_u$  GOS ratio-ed to the computed GOS for the  $2\pi_u^*$  GOS. The residual signal is less than 1% of the ratio signal, so it is not too surprising that the experimental signal is still somewhat noisy. However, there is clearly an oscillatory component with a shape and amplitude rather similar to the computed signal. Note that the experimental signal has been inverted to achieve the match to the computed signal.

Fig. 5b also shows the computed oscillatory component in the  $3s\sigma_g$  GOS. This is more regular and about two times more intense than that in the 539 eV signal since the latter is damped because of the out-of-phase character of the  $4s\sigma_g$  and  $3p\sigma_u$  contributions. Since the 3s signal does not overlap other predicted states with oscillatory GOS profiles, it would be a better candidate to experimentally verify this interesting effect. However, even at high resolution [12], the  $3s\sigma_g$  state is only a weak high energy shoulder on the strong  $\pi^*$  peak. The energy resolution used for these measurements was not sufficient to reliably isolate the  $3s\sigma_g$  signal from the much stronger, and overlapping  $2\pi_u^*$ .

Further theoretical and experimental work is needed to better understand the origin of these oscillations. In addition to the computational studies in progress, we intend to use our spectrometer in monochromatic mode to measure the O  $1s \rightarrow 3s\sigma_g$  signal as well as the 539 eV signal at higher statistical precision.

## Acknowledgements

This research is supported financially by NSERC (Canada), CAPES, FAPERJ, FUJB and CNPq (Brazil).

## References

- [1] I.G. Eustatiu, T. Tyliczszak, A.P. Hitchcock, C.C. Turci, A.B. Rocha, C.E. Bielschowsky, *Phys. Rev. A* 61 (2000) 042505.
- [2] I.G. Eustatiu, J.T. Francis, T. Tyliczszak, C.C. Turci, A.L.D. Kilcoyne, A.P. Hitchcock, *Chem. Phys.* 257 (2000) 235.
- [3] V.N. Sivkov, V.N. Akimov, A.S. Vinogradov, T.M. Zimkina, *Opt. Spectrosc. USSR* 57 (1984) 160.
- [4] A.P. Hitchcock, J. Stöhr, *J. Chem. Phys.* 87 (1987) 3253.
- [5] A.B. da Rocha, I. Borges Jr., C.E. Bielschowsky, *Phys. Rev.* 57 (1998) 4394.
- [6] C.E. Bielschowsky, G.G.B. de Souza, C.A. Lucas, H.M. Boechat Roberty, *Phys. Rev. A* 38 (1988) 3405.
- [7] M.P. de Miranda, C.E. Bielschowsky, M.A.C. Nascimento, *J. Phys. B* 28 (1995) L15.
- [8] D.A. Swick, *Rev. Sci. Instr.* 31 (1960) 525.
- [9] J. Karle, *J. Chem. Phys.* 35 (1961) 963.
- [10] J. Karle, D.A. Swick, *J. Chem. Phys.* 35 (1961) 2257.
- [11] J.S. Lee, T.C. Wong, R.A. Bonham, *J. Chem. Phys.* 4 (1975) 1609.
- [12] M.N. Piancastelli, A. Kivimäki, B. Kempgens, M. Neeb, K. Maier, A.M. Bradshaw, *Chem. Phys. Lett.* 274 (1997) 13.